



# An assessment of radionuclides level, radon and thoron exhalation rate in hill and field soil of Mahendergarh district in Haryana, India

Kavita Chahal<sup>1</sup> · Suneel Kumar<sup>1</sup> · Savita Budhwar<sup>2</sup> · Amanjeet<sup>3</sup> · Ranjeet Singh<sup>4</sup> · Balvinder Singh<sup>4</sup>

Received: 21 November 2023 / Accepted: 7 April 2024 / Published online: 10 May 2024  
© Akadémiai Kiadó, Budapest, Hungary 2024

## Abstract

To investigate the activity concentrations of naturally occurring radionuclides such as  $^{238}\text{U}$ ,  $^{232}\text{Th}$ , and  $^{40}\text{K}$ , as well as the presence of radon ( $^{222}\text{Rn}$ ) and thoron ( $^{220}\text{Rn}$ ) in the vicinity of the Aravalli Mountain range in Mahendergarh, India, a comprehensive study was conducted. We meticulously examined soil samples obtained from both field and hill areas using NaI (TI) detector based on gamma spectroscopy. It is noteworthy that concentrations were found lower than the global average values. Notably, the hill soil samples exhibited a higher activity concentration in comparison to the field soil samples. Overall, in terms of radium equivalent activity ( $^{226}\text{Ra}$ ), gamma absorbed dose rate, and the internal hazard index, our findings did not reveal any significant radiological risks.

**Keywords** Naturally occurring radionuclides · Smart RnDuo radon monitor · Hill soil · Exhalation rates · Aravalli mountain range

## Introduction

Soil is the principal reservoir for all essential life supporting components either directly or indirectly. It contributes significantly to the natural background radiation and these radiations exposed to the surroundings [1, 2]. Soil constitutes the uppermost layer of the earth crust, formed through a series of physiochemical changes including decomposition, water movement, and weathering of solid rock. Within the earth crust, rocks and minerals naturally emit low levels of radiation due to the presence of radioactive isotopes. Soil comprises minerals and rocks that naturally erode, releasing radioactive elements, particularly uranium ( $^{238}\text{U}$ ), thorium ( $^{232}\text{Th}$ ), and potassium ( $^{40}\text{K}$ ), along with their decay

products, as inherent components of soil. Radiation is an integral aspect of our environment, and human exposure and radiation occurs through routine interactions, such as exposure to sunlight and natural background radiation [3].

Background radiation encompasses cosmic radiation that constantly permeates the atmosphere from space. The average annual natural background radiation exposure for humans is approximately 1.1 mSv, sourced from cosmic radiation (0.35 mSv) and from atmospheric sources its value is 0.05 mSv [4]. The distribution of radionuclides in soil and their radiological impacts significantly influence human health. These radionuclides account for at least 80% of natural radiation exposure [5, 6], with the remaining 20% stemming from human activities. Elevated levels of anthropogenic radiation, originating from  $^{238}\text{U}$  and its decay products in geological materials as well as  $^{232}\text{Th}$ , predominantly found in zircons, igneous rocks, and monazite sands are significant contributors to high background radiation levels. In some regions, the presence of monazite sands has resulted in exceptionally high background radiation levels, increasing radiation exposure in various countries [7–15]. Pegmatite, granite, diorite, and gneiss rock samples of North Pakistan were highly radioactive and should not be used as constructing material [16]. Globally, naturally the high background radiation place is Ramsar City, Iran. In Iran, high background radiation is due to the presence

✉ Suneel Kumar  
suneelkumar@cuh.ac.in

<sup>1</sup> Department of Physics & Astrophysics, Central University of Haryana, Mahendergarh, Haryana 123031, India

<sup>2</sup> Department of Nutrition Biology, Central University of Haryana, Mahendergarh, Haryana 123031, India

<sup>3</sup> Department of Physics, Ramjas College, University of Delhi, New Delhi, Delhi, India 110007

<sup>4</sup> Department of Physics, Centre of Radio Ecology, Guru Jambheshwar University of Science and Technology, Hisar 125001, India

of  $^{226}\text{Ra}$  in local rocks [17]. Mrima Hill of Kenya country, known for high background radiation due to the presence of heavy minerals like carbonatites, and monazites. Here, activity concentration of naturally occurring radioactive elements and dose rate were found above the global value [18]. Also, in India, Kerala has a high level of radiation, and the attribution of radiation is due to monazite sand containing enriched thorium [8]. Prior research has shown that higher levels of radon and thoron in the environment significantly increase the risk of lung cancer even in non smokers [19–24]. Radon ( $^{222}\text{Rn}$ ) and thoron ( $^{220}\text{Rn}$ ) are released from soil and construction materials into the environment through emanation and exhalation. The exhalation rate is influenced by various factors, including the content of  $^{226}\text{Ra}$  in the soil, rock composition, porosity, permeability, temperature, humidity, and meteorological conditions [25–28]. Thus, this study project also included the measurement of the exhalation rate for soil samples to assess potential health risks.

Although radionuclide levels in soil have been measured in various regions of Haryana over the past few decades [28–32]. No prior investigations have been reported on these radioactive elements in the soils of the Mahendergarh district in Haryana. Given the common association of  $^{238}\text{U}$  and  $^{232}\text{Th}$  with the Aravalli Hills, radiation exposure from this region could be an environmental concern. Consequently, it is essential to conduct a qualitative analysis of these radionuclides in this specific research area. Buildings in India commonly utilize bricks that incorporate approximately 80% soil [20]. Therefore, this study aims to determine whether the soil in this area is suitable for construction without posing risks to human health.

Radionuclide  $^{226}\text{Ra}$  is known to migrate more readily in the environment and its decay product, radon gas escapes from the soil. While various natural radionuclides such as those in the  $^{235}\text{U}$  series,  $^{176}\text{Lu}$ ,  $^{87}\text{Rb}$ , and  $^{147}\text{Sm}$  exist in the environment at low levels and their contributions to human radiation exposure are relatively low [33]. As a result, this study focuses on the assessment of radionuclides  $^{238}\text{U}$ ,  $^{232}\text{Th}$ , and primordial radionuclide  $^{40}\text{K}$  in the soil, utilizing a gamma ray spectrometer to measure element activity concentrations and calculate the exhalation rates of  $^{222}\text{Rn}$  and  $^{220}\text{Rn}$  for the soil samples by employing the SMART RnDuo portable radon monitor.

## Geological characteristics of the study area

The research was conducted in the vicinity of the Aravalli Mountain range located in Mahendergarh, Haryana, India. This district spans between  $24^{\circ} 47'$  to  $28^{\circ} 26'$  N latitudes and  $75^{\circ} 56'$  to  $76^{\circ} 51'$  E longitudes, covering an area of  $1899 \text{ km}^2$ . The region primarily falls within the Indo Gangetic plains geomorphological zone.

The predominant soil types in this district include arid soil, blown sand, and alluvium. These soils typically contain subsurface lime nodules and exhibit calcareous characteristics. The geological substrata of the district consist of rocks belonging to the Delhi and Delhi systems, overlain by recent alluvial deposits and blown sand.

The area surrounding the district features prominent hill formations, notably the Madhogarh Hill, Dhosi Hill, and the Tosham Hill range. These hills are situated within the Aravalli Mountain range and primarily consist of meta-sedimentary rocks [34]. These metasedimentary rocks predominantly comprise quartzite and contain a relatively low number of pegmatites, slate granite, and phyllite. The Tosham Hill range, an essential component of the Aravalli Mountain range, falls under the Archean Bilwala basement rock category and primarily comprises quartz and granite porphyries known for their high thermal conductivity.

Climatically, the study area experiences an annual average rainfall of approximately 500 mm, with uneven distribution across the region. Moreover, the district is situated near the Dohan River, which is currently facing the threat of extinction. The Krishnavati River originates from the Aravalli range, near the Dariba copper mine in the state of Rajasthan.

## Experimental procedure

### Sample preparation

In this research, a total of 28 soil samples were initially chosen randomly from various surface areas, including rock formations within the Aravalli range, for the determination of radionuclides. Subsequently, 17 of these soil samples were selected for the measurement of radon and thoron exhalation rates in Mahendergarh, Haryana, India, as illustrated in Fig. 1. Each sample was obtained at a depth of 45 cm and was accurately positioned using GPS coordinates.

The collected samples, each weighing approximately 1 kg, underwent a series of processing steps, including grinding, sieving, and homogenization, resulting in a particle size of 100 mesh, achieved through the use of a crushing machine. Following this, the prepared samples were dried at  $110^{\circ}\text{C}$  for 12 h to ensure the complete removal of moisture. After the samples were weighed, they were placed into sun pet jars, hermetically sealed, and left undisturbed for over one month. This critical step allowed for the establishment of secular equilibrium, as described in previous studies [35, 36]. By doing so, it ensured that radon gas was contained within the samples, and its decay products remained within the samples for subsequent measurements and analysis.

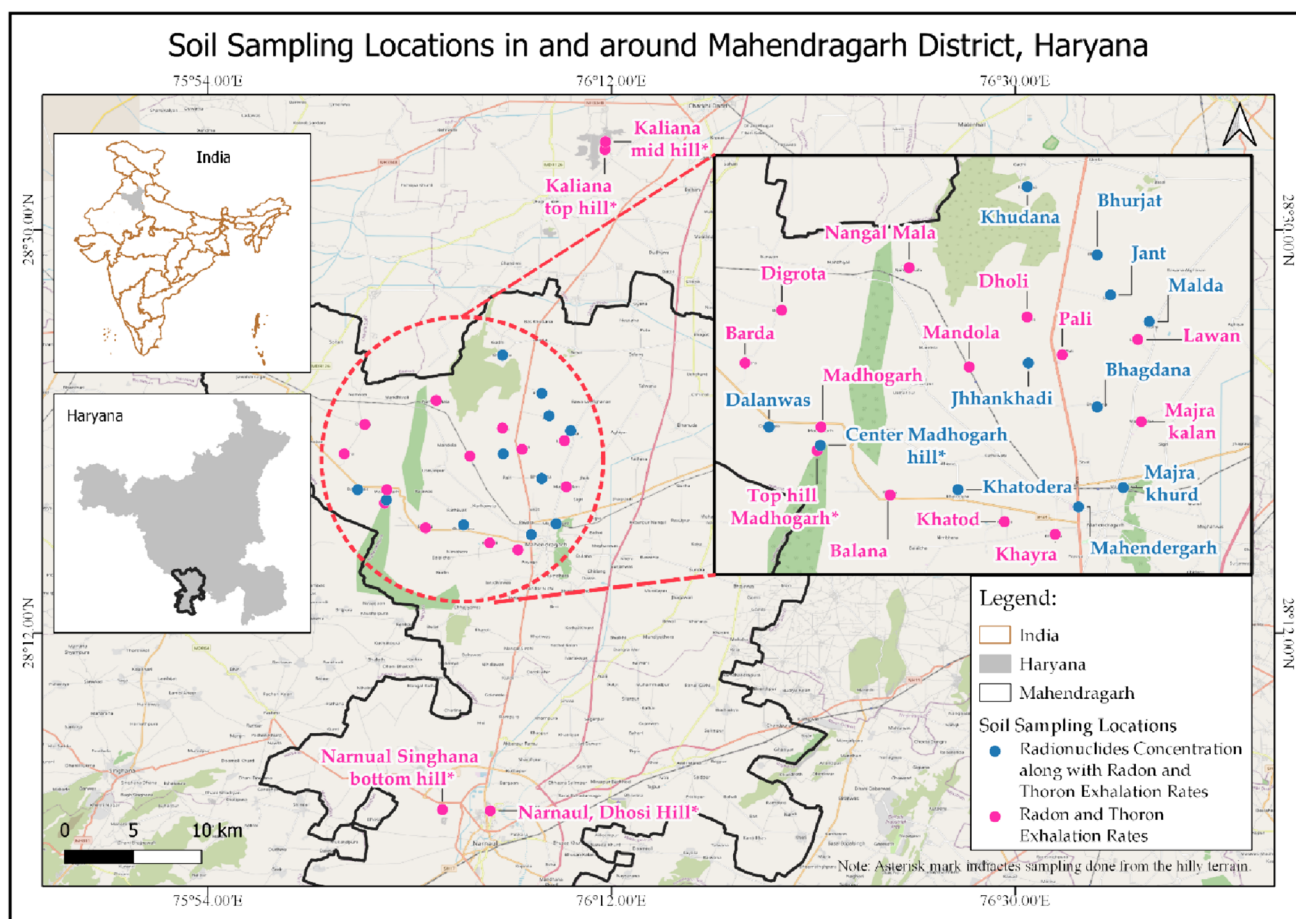


**Fig. 1** Surveyed area map for soil samples in Mahendragarh, district, Haryana India

### Instrumentation and calibration

For the determination of the concentration of natural radionuclides, a  $\gamma$ -ray spectrometer employing NaI (TI) scintillation detector with dimensions of  $2'' \times 2''$  was utilized. The detector (MODEL: NETS – ØM) was supplied by electronic enterprises (I) PVT. Ltd PARA Electronics-Mfg. Division Mulund Mumbai. The detector boasts a resolution of (FWHM) 1.85 keV for the 1.33 MeV gamma line of  $^{60}\text{Co}$  [37]. Energy calibration was performed using point sources of  $^{60}\text{Co}$  and  $^{137}\text{Cs}$ .

### Measurement of radioactivity concentration

The measurement of radioactivity concentration involved the use of  $\gamma$ -rays emitted by specific radioactive isotopes for analysis. Notably, the  $\gamma$ -rays of interest included 186.2 keV for  $^{238}\text{U}$ , 911 keV, 968 keV for  $^{232}\text{Th}$ , and 1460.8 keV for  $^{40}\text{K}$  [38]. The counting period for each sample was set at 80,000 s to ensure robust statistical data. Subsequent analysis of the obtained counts facilitated the calculation of the

activity concentration of radioactive elements, specifically  $^{238}\text{U}$ ,  $^{232}\text{Th}$ , and  $^{40}\text{K}$  reported in Bq/kg.

### Theoretical calculations

Given the non-uniform distribution of natural radionuclides ( $^{238}\text{U}$ ,  $^{232}\text{Th}$ , and  $^{40}\text{K}$ ) within the soil, an assessment of radiological risks associated with soil usage was performed using a single index incorporating the activity of various radionuclides. The activity concentrations of uranium, potassium, and thorium were calculated employing the following Eq. (1) [39, 40].

$$\text{Activity concentration (Bq kg}^{-1}\text{)} = \frac{\text{Net count rate}}{\text{efficiency} \times \text{sample weight} \times \text{abundance}} \quad (1)$$

Radium ( $\text{Ra}_{\text{eq}}$ ) equivalent activity is used to compute the total radiation exposure caused by radionuclides ( $^{238}\text{U}$ ,  $^{232}\text{Th}$ , and  $^{40}\text{K}$ ). The calculation is performed by using the following Eq. (2) [38, 41, 42].

$$Ra_{eq}(\text{Bq kg}^{-1}) = A_U(\text{Bq kg}^{-1}) + 1.43 A_{Th}(\text{Bq kg}^{-1}) + 0.077 A_K(\text{Bq kg}^{-1}) \quad (2)$$

where  $A_U$ ,  $A_{Th}$ , and  $A_K$  are the concentrations of  $^{238}\text{U}$ ,  $^{232}\text{Th}$ , and  $^{40}\text{K}$  in  $\text{Bq kg}^{-1}$  respectively [7].

### Hazard index

Internal hazard index ( $H_{in}$ ) measures the effect of radionuclides on the lungs and other organs. Its value must be less than unity. Using the following Eq. (3), one can determine the risks due to naturally occurring radionuclides [42].

$$H_{in} = \frac{A_U}{185} + \frac{A_{Th}}{259} + \frac{A_K}{4810} \quad (3)$$

The constant terms are used, it is assumed that the radiation doses for  $^{238}\text{U}$ ,  $^{232}\text{Th}$ , and  $^{40}\text{K}$  were  $185 \text{ Bq kg}^{-1}$ ,  $259 \text{ Bq kg}^{-1}$ , and  $4810 \text{ Bq kg}^{-1}$  to provide equal gamma radiation dose [43, 44].

### Absorbed dose rate (AAD)

It can be calculated by using the following Eq. (4) [7] using activity concentrations of  $^{238}\text{U}$ ,  $^{232}\text{Th}$ , and  $^{40}\text{K}$  (UNSCEAR 2000).

$$AAD(\text{nGyh}^{-1}) = 0.462 A_U(\text{Bq kg}^{-1}) + 0.604 A_{Th}(\text{Bq kg}^{-1}) + 0.0417 A_K(\text{Bq kg}^{-1}) \quad (4)$$

where  $A_U$ ,  $A_{Th}$ , and  $A_K$  are the radioactivity concentrations of natural radionuclides in soil samples [45].

### Radon exhalation rate measurement

To determine the exhalation rate of  $^{222}\text{Rn}$  in soil samples, a Portable Radon Monitor developed by BARC (Bhabha Atomic Research Centre) was employed, as depicted in

Fig. 2. This monitor operates by detecting alpha particles produced by  $^{222}\text{Rn}$  and its progenies, namely  $^{218}\text{Pb}$  and  $^{214}\text{Po}$ .

The procedure involved placing the soil sample within a stainless steel cylindrical container with a known weight ( $M$ ). The container measured 8.2 cm in height and had an inner diameter of 10 cm. A progeny filter was utilized to selectively collect radon while effectively eliminating the  $^{222}\text{Rn}$  descendants. In addition, a pinhole plate was employed to suppress thoron, which is relatively short lived. This step was essential to account for the diffusion time delay, a phenomenon in which the transmission of  $^{220}\text{Rn}$  takes longer compared to radon transmission due to the shorter lifetime of thoron. Each measurement was carried out for 9 h to ensure a comprehensive assessment of the accuracy and precision of the experimental setup, a quality control measure verified by the creator of the SMART RnDuo [46].

The radon mass exhalation ( $J_m$ ) rate is calculated by analysing the radon concentration  $C(t)$ , and applying Eq. (5) [46–50].

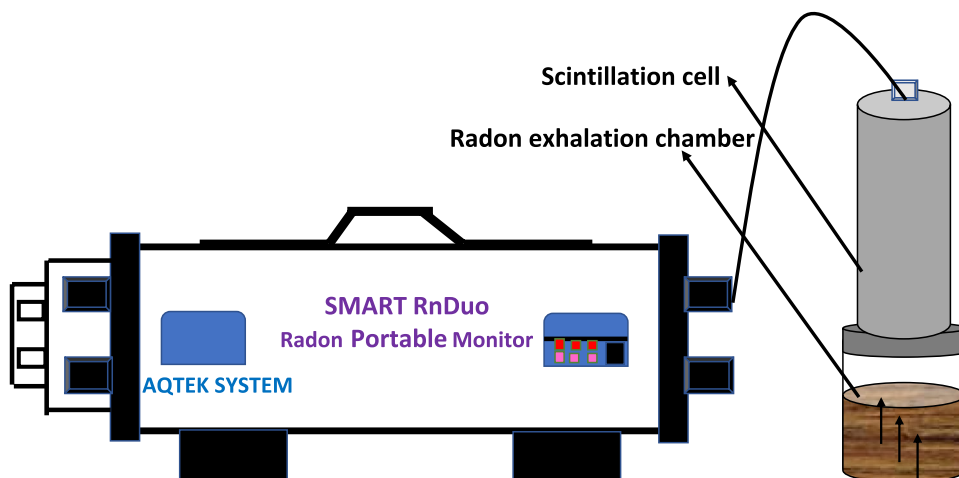
$$C(t) = \frac{J_m M}{V \lambda_e} (1 - e^{-\lambda_e t}) + C_0 e^{-\lambda_e t} \quad (5)$$

where  $J_m$  is the radon mass exhalation rate in  $\text{mBq/kg/h}$ ,  $V (\text{m}^3)$  is the sum of the effective chamber volume and the volume of the scintillation cell,  $M (\text{kg})$  is the sample mass,  $\lambda_e (\text{h}^{-1})$  is the effective decay constant due to decomposition of  $^{222}\text{Rn}$ , back diffusion, leakage rate of chamber,  $C_0$  is the initial radon concentration in the chamber at time  $t = 0$ .

### Measurement of thoron surface exhalation rate

To assess the concentration of  $^{220}\text{Th}$ , a flow mode sampler was connected to the inlet of the monitor as shown in Fig. 3. This sampler was exclusively used for the quantification of thoron. The quantification process involved a 15 min cycle during which measurements of thoron levels

**Fig. 2** Experimental set up used for the assessment of  $^{222}\text{Th}$  exhalation rate in soil samples



and background counts were recorded. Following this cycle, a 5 min hold up period was observed to ensure that the  $^{220}\text{Th}$  had nearly completely decayed. Subsequently, a final 5 min count was conducted to determine the number of background counts associated with that specific cycle.

The surface rate ( $J_{st}$ ) of thoron in  $\text{Bq}/\text{m}^2/\text{s}$  was calculated using Eq. (6), as previously employed and validated in related studies [51–53].

$$J_{st} = C_t \frac{V\lambda}{A} \quad (6)$$

where  $C_t$  is the build up  $^{220}\text{Rn}$  concentration ( $\text{Bq}/\text{m}^3$ ) within the chamber as determined by a portable monitor throughout 15 min cycle.  $V$  ( $\text{m}^3$ ) is the leftover air volume enclosed by the loop.  $A$  ( $\text{m}^2$ ) is the sample surface area.  $\lambda$  is the decay constant of  $^{220}\text{Rn}$  ( $0.012464 \text{ s}^{-1}$ ).

## Results and discussion

### Naturally occurring radionuclides

Using NaI (Tl) detector, the radioactivity concentration in the study area was determined. The activity concentration of  $^{238}\text{U}$ ,  $^{232}\text{Th}$ , and  $^{40}\text{K}$  varied within the range of (0.06–1.81)  $\text{Bq}/\text{kg}$ , (0.09–2.37)  $\text{Bq}/\text{kg}$ , and (3.09–10.9)  $\text{Bq}/\text{kg}$  with mean values of 0.84  $\text{Bq}/\text{kg}$ , 1.16  $\text{Bq}/\text{kg}$ , and 7.08  $\text{Bq}/\text{kg}$ , respectively. It is noteworthy that these activity concentrations of  $^{238}\text{U}$ ,  $^{232}\text{Th}$ ,  $^{40}\text{K}$ , and  $^{226}\text{Ra}_{\text{eq}}$  radionuclides are below the permissible limits of the world average values of 32  $\text{Bq}/\text{kg}$ , 30  $\text{Bq}/\text{kg}$ , 400  $\text{Bq}/\text{kg}$ , and 370  $\text{Bq}/\text{kg}$ , as outlined by UNSCEAR in 2000.

The coefficient of variability was highest for  $^{238}\text{U}$  (49%) and lowest for  $^{40}\text{K}$  (23%). Notably, the highest concentrations of uranium, thorium, and potassium were found in Jhankhadi village, Narnaul Singhana bottom hill, and Narnaul Dhosi hill, while the maximum radium equivalent activity concentration was observed in Narnaul Singhana bottom hill.

Analysis of Fig. 4 reveals that the activity concentration of  $^{40}\text{K}$  in all soil samples was greater than that of  $^{238}\text{U}$  and  $^{232}\text{Th}$ , which is consistent with soil expectations. This variation may be attributed to geological disparities, the application of chemical fertilizers for agricultural purposes, and the presence of the Aravalli Hills, all contributing to the increased radioactivity in the study area.

Furthermore, as illustrated in Fig. 4 the activity concentration of  $^{232}\text{Th}$  surpasses that of  $^{238}\text{U}$  in all soil samples, except for seven locations. This finding suggests the prevalence of thorium rich soil in the study area, corroborating the

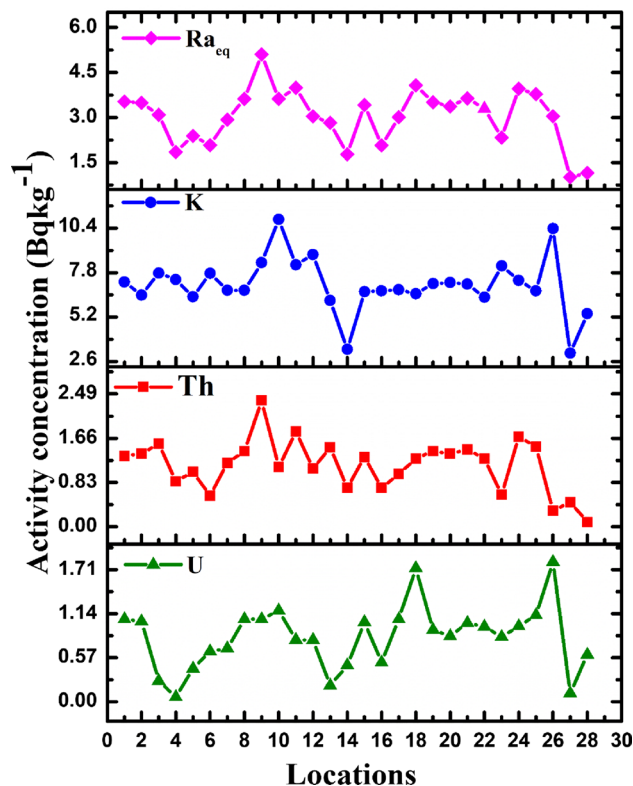
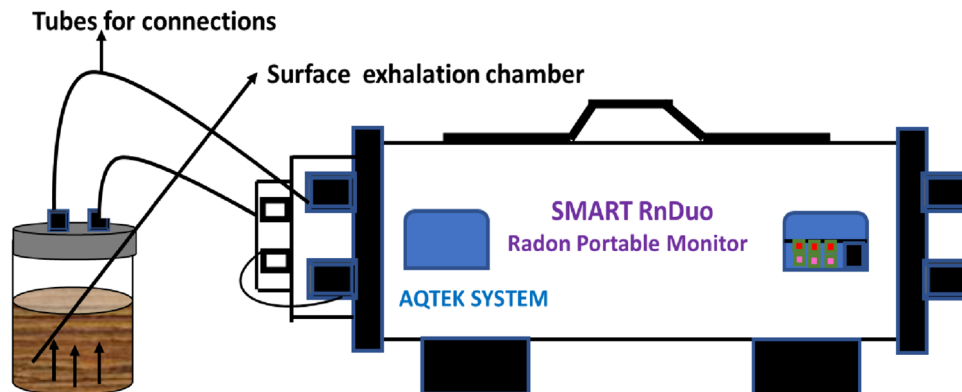


Fig. 4 Variations of radioactive nuclides activity content in soil samples

Fig. 3 Experimental set up used for the assessment of  $^{220}\text{Th}$  exhalation rate in soil samples



notion that thorium is more abundant in nature than uranium, in alignment with the World Nuclear Association Report in 2020 on thorium. The contribution of radionuclides to the absorbed dose rate in air depends on their concentration in the soil, with absorbed dose rates varying from 0.46

to 2.28 nGy/h, averaging 1.38 nGy/h. In comparison to the world average absorbed dose rate of 86 nGy/h (UNSCEAR, 2000), the calculated values in the soil samples are significantly lower, underscoring the region safety in terms of radiation exposure. Additionally, the calculated average value of the internal hazard index ( $H_{in}$ ) was determined to be 0.01, indicating values lower than the safe threshold.

**Table 1** Radon mass exhalation rate at survey site areas

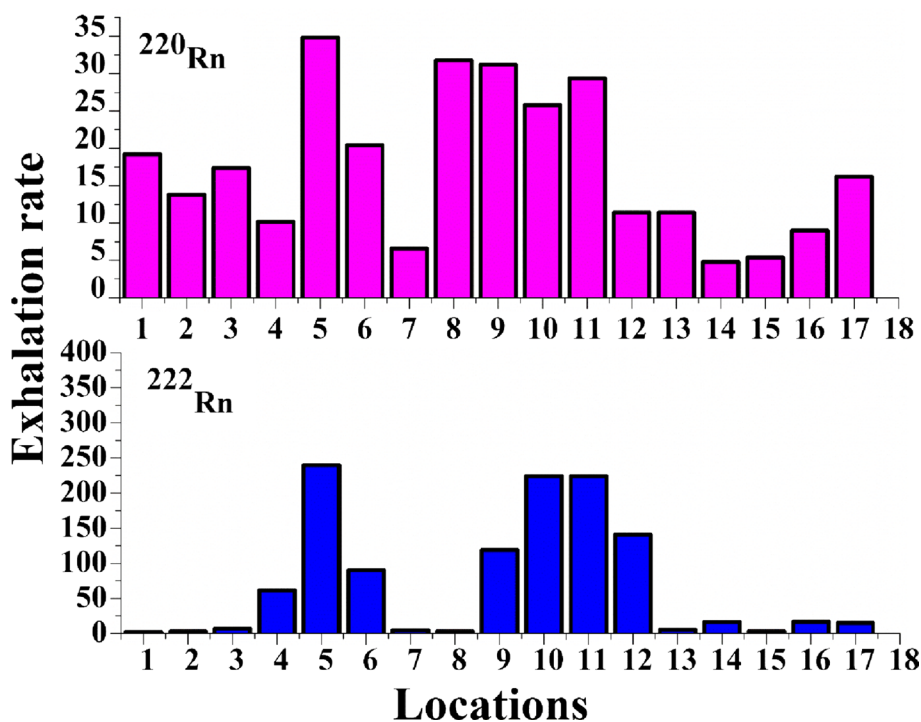
Locations	Radon exhalation rate (mBq/kg/h)	Thoron surface exhalation rate (Bq/m <sup>2</sup> /h)
Lawan, field soil	1.96	19.2
Majra Kalan, field soil	2.68	13.8
Khayra, field soil	7.05	17.4
Khatod, field soil	61.4	10.2
Madhogarh, mid hill soil	240	34.8
Madhogarh, top hill soil	90	20.4
Barda, field soil	4.38	6.6
Pali, field soil	2.99	31.8
Narnaul Singhana hill soil	119	31.2
Narnaul, Dhosi hill soil	224	25.8
Kaliana, mid hill soil	224	29.4
Kaliana, top hill soil	141	11.4
Mandola, field soil	5.4	11.4
Dholi, field soil	16.4	4.8
Digrota, field soil	3.01	5.4
Nangal Mala, field soil	16.9	9.0
Balana, field soil	14.7	16.2
Mean	51.9	17.4

### Radon and Thoron exhalation rate

The mean values of <sup>222</sup>Rn mass and <sup>220</sup>Rn surface exhalation rate were found to be 51.9 and 17.4 Bq/m<sup>2</sup>/h, respectively as reported in Table 1. The mean value of radon mass exhalation rate is approximately 9% lower than the world average value of 57 mBq/kg/h, while the mean value of thoron surface exhalation rate is nearly 99.5% lower than the world average value of 3600 Bq/m<sup>2</sup>/h, as reported by UNSCEAR in 2000.

In the bar graph presented in Fig. 5 and Table 1, it is evident that the maximum thoron exhalation rate was recorded for Madhogarh Mid Hill (location no. 5), measuring 34.8 Bq/m<sup>2</sup>/h, while the maximum mass exhalation rate of 240 mBq/kg/h was also found in Madhogarh Mid Hill. The figure illustrates high peaks representing rock samples and lower peaks representing field area samples. Specifically, the samples with sample numbers 5, 6, 9, 10, 11, and 12 correspond to hill soil samples, exhibiting higher radon mass and thoron surface exhalation rates compared to the rest of the samples, which are field soil samples.

**Fig. 5** Radon mass and Thoron surface exhalation rate in soil samples of the area under study



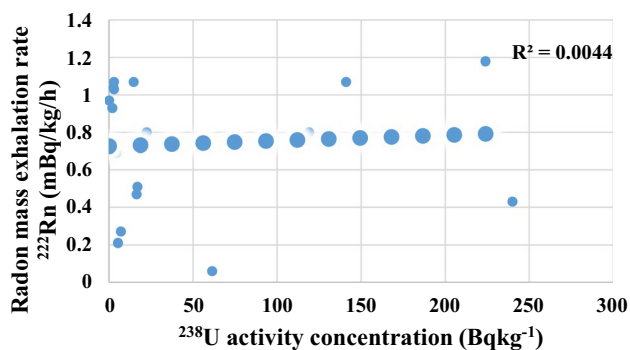


**Fig. 6** Correlation between  $^{222}\text{Rn}$  mass exhalation rate and  $^{238}\text{U}$  activity concentration

### Correlation between radionuclides present in soil samples

Figure 6 illustrates the correlation between  $^{238}\text{U}$  and  $^{222}\text{Rn}$ , which is weak but positive, with an  $R^2$  value of 0.0044. As demonstrated in Fig. 7, thorium exhibits a weak yet positive correlation (0.0299) with thoron. It is important to note that no strong statistical relationship exists between these radionuclides, indicating that the radioactive content in soil samples is influenced by the diverse nature of these radionuclides. Therefore, the distribution of one radionuclide in

**Fig. 7** Correlation between  $^{220}\text{Th}$  surface exhalation rate and  $^{232}\text{Th}$  activity concentration

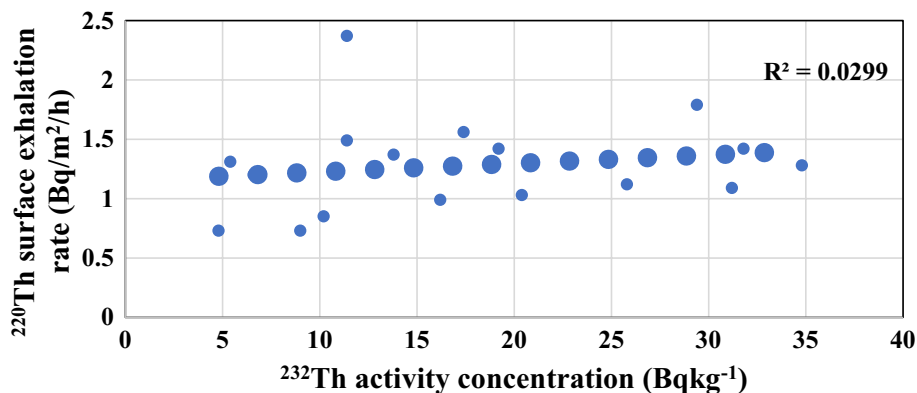


**Table 2** Comparative study of surveyed area with India hilly areas

Hilly areas	Radon exhalation rate (mBq/kg/h)		References
	Min	Max	
Kamaun hills region, Uttarakhand	16	54	Semwal et al. [55]
Sub mountainous region, J & K	15 ± 0.4	38 ± 0.8	Kaur et al. [56]
Siwalik hills Himalaya, Jammu & Kashmir	7 ± 0.6	48 ± 1.3	Kaur et al. [57]
Himalaya foothills region, Uttarakhand	16	111	Anamika et al. [7]
Granitic hills region, Karnataka	76 ± 6	269 ± 19	Poojitha et al. [54]
Shivalik hills, Haryana & Himachal Pradesh India	50 ± 1	143 ± 6	Chauhan et al. [58]
Aravalli hills, Mahendergarh Haryana	1.96	240	Present study

the soil does not depend on the concentration of another radioactive element.

To further contextualize the results, the study area was compared with hilly areas in India, particularly those surrounded by the Aravalli hills, as shown in Table 2. The findings revealed that the radon exhalation rate in the study area was similar to that of Granitic hills in Karnataka [54]. However, the values for radon exhalation rate were lower in comparison to Kamaun Hills in Uttarakhand [55], sub-mountainous regions in Jammu & Kashmir [56], Shivalik Hills in Himalaya [57], the Himalaya foothill region in Uttarakhand [7] and Shivalik Hills in Haryana and Himachal Pradesh [58].

### Differentiation of natural radioactivity in rock soil samples

The natural hills in the study area, such as Madhogarh, Dhosi, Kaliaana, and Singhana Hills are formed through various geological processes. These hills can also result from erosion, where rocks, soil, and sediments accumulate in a particular area. The presence of natural radionuclides and the exhalation of  $^{222}\text{Rn}$  and  $^{220}\text{Rn}$  were found to be greater in hill soil samples as compared to field samples. The statistical data plotted for gamma absorbed dose rate values and hazard index is presented in Fig. 8. Here, the maximum hazard

index and absorbed dose rate were found for Narnaul Singhana Bottom Hill. The distribution of radionuclides in hill soil samples is depicted in Fig. 9, where it can be observed that the activity concentration of  $^{238}\text{U}$  was highest for Dhosi Hill,  $^{232}\text{Th}$  was most prominent in Narnaul Singhana Hill,  $^{40}\text{K}$  concentration was at its peak in Dhosi Hill, and  $^{220}\text{Rn}$  and  $^{222}\text{Rn}$  were elevated in Madhogarh Mid Hill soil samples. Narnaul Dhosi Hill predominantly consists of quartzite, with some pegmatite, slate, granite gneiss, phyllite, schist, and various basic rocks. The sharp contact between pegmatite and quartzite, along with the blurred contact between granite and pegmatite at Narnaul, serve as strong evidence of geological movement within the Aravalli orogenic belt [59]. The high concentration of heat producing elements in granite indicates the presence of radioactive elements like  $^{238}\text{U}$ ,  $^{232}\text{Th}$ , and  $^{40}\text{K}$ . Madhogarh Hill, an isolated hill within the Aravalli range, is believed to release significant amounts of radon and thoron gases due to the presence of basic rocks.

Rocks found in the Kaliana Hills predominantly consist of mica, quartz grains, sedimentary quartzite, and flexible sandstone known as Itacolumite. While both flexible and non flexible sandstone can be found in the Kaliana area, non flexible sandstone is more abundant relative to flexible sandstone. Cementing materials such as floor tiles are produced

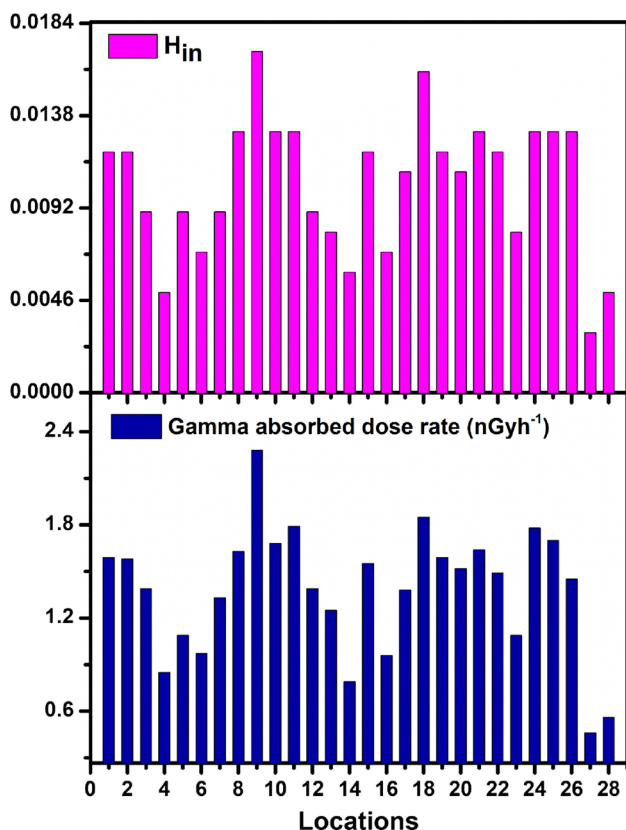


**Fig. 8** Gamma absorbed dose rate and hazard index ( $H_{in}$ ) for various locations of the studied area

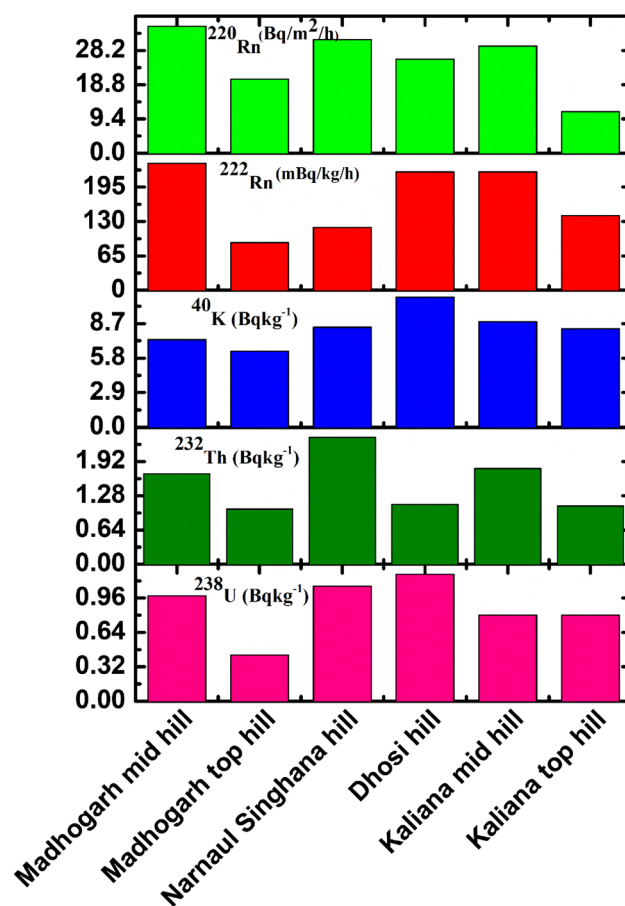


**Fig. 9** Distribution of naturally occurring radionuclides material ( $^{238}\text{U}$ ,  $^{232}\text{Th}$ ,  $^{40}\text{K}$ ) and exhalation rate in different rock samples

using these sandstones. Although the concentration of radionuclides was higher in Kaliana Hill as compared to field soil, it remained within safe limits. This suggests that Kaliana soil samples can be utilized for building materials [60]. Narnaul Singhana Hill is part of parametamorphites belonging to the Delhi Subdivision, and it is characterized by schists, amphibole quartzite, and mineralized shear zones. These features may account for the high concentration of thorium in the area. Additionally, inhomogeneity in the distribution of radioactive elements in different geological layers of the hill was observed, with some layers being more radioactive than others. This variation is attributed to temperature differences at different elevations of the hill, with the top elevation having lower temperatures than the midsection. The distribution of radioactive elements is also influenced by the type of rock in a given layer, emphasizing the need for future researchers to conduct radiometric measurements at specific hill locations.

Certain types of hills, such as those with sedimentary rocks like Kaliana Hill, exhibit lower radioactivity concentrations in comparison to hills containing granites and some



metamorphic rocks. As demonstrated in Fig. 9, Kalia Hill did not have the highest radionuclide concentrations, as it primarily consists of sedimentary rocks. According to the literature survey, sedimentary rocks consist of low radioactivity as compared to igneous rocks [61]. Deposition, soil erosion, and topographical variations affect the morphological, chemical, and physical characteristics of the soil [62]. In hilly areas, the radioactivity is high which is interrelated with dental fluorosis [63]. Mahendergarh area is also a fluorosis endemic red zone alert area, here fluoride distribution in groundwater is due to fluoride bearing rocks. Here dental fluorosis was diagnosed, and found high level of fluoride [64]. The present area is an industries free, pollution free area, and inhabitants of this area are dependent on agriculture. So, industrial aerosols are not responsible for high radioactivity in this area. This is the reason that there is no radioactivity was found in the field soil samples. Also, one can say that the geology of this area, and radiation bearing rocks may be responsible for high activity concentration in hills soil samples.

## Conclusions

In conclusion, the activity concentration values in the study area are influenced by geographical conditions, soil composition, and the presence of the Aravalli hills. These values were found to be lower than the world average, indicating that the radiation levels in the area are within safe limits. Additionally, the prevalence of higher  $^{232}\text{Th}$  concentration over  $^{238}\text{U}$  in all samples suggests that the soil in the study region is thorium enriched. The hills with granite and gneiss rocks exhibited the highest radioactivity concentrations, whereas sandstone rocks had lower concentrations. When compared to the world average absorbed dose rate, the calculated values suggest that the study area is safe in terms of radiation levels. As this study is the first of its kind, it holds importance for future researchers in the field of natural radioactivity mapping and radiometric measurements in hilly areas. In summary, the results of this study indicate that the soil in both hill and field areas is suitable for use in construction materials and does not pose any health risks to residents.

**Acknowledgements** The authors are thankful to the inhabitants of the studied area for their cooperation during the fieldwork and thankful to the Guru Jambheshwar University of Science and Technology, Hisar for providing experimental facilities and support. One of the authors Kavita Chahal thankful to Central University of Haryana for providing a Research fellowship.

## Declarations

**Conflict of interest** The authors declare that they have no known conflicting financial interests or personal relationships that could have ap-

peared to influence the findings represented in this paper. The authors declare that there is no conflict of interest in the publication of the paper.

## References

1. UNSCEAR (1988) Sources, effects and risks of ionizing radiation. United Nations Scientific Committee on the Effects of Atomic Radiation, Report to the General Assembly
2. Kumar M (2022) Estimation of  $^{222}\text{Rn}$ ,  $^{220}\text{Rn}$  exhalation rate and  $^{226}\text{Ra}$ ,  $^{232}\text{Th}$ ,  $^{40}\text{K}$  radionuclides in the soil samples of different regions of Gurdaspur district, Punjab. *Mater Today Proc* 49:3396–3402
3. Alzubaidi G (2016) Assessment of natural radioactivity levels and radiation hazards in agricultural and virgin soil in the state of Kedah, North of Malaysia. *Sci World J*. <https://doi.org/10.1155/2016/6178103>
4. Johnson S (1991) Natural radiation. *Va Miner* 37(2):9–16
5. International Atomic Energy Agency (1973) Regulations for the safe transport of radioactive materials. 96–00725 IAEA/PI/A47E
6. United Nations Scientific Committee on the Effect of Atomic Radiation (UNSCEAR) (1993) Exposure from natural sources of radiation, United Nations, New York
7. Anamika K (2020) Assessment of radiological impacts of natural radionuclides and radon exhalation rate measured in the soil samples of Himalayan foothills of Uttarakhand, India. *J Radioanal Nucl Chem* 323:263–274. <https://doi.org/10.1007/s10967-019-06876-0>
8. Venunathan N (2016) Natural radioactivity in sediments and river bank soil of Kallada river of Kerala, South India and associated radiological risk. *Radiat Prot Dosimetry* 171(2):271–276. <https://doi.org/10.1093/rpd/ncw073>
9. Bennett B (1996) Exposure to natural radiation worldwide. In: Proceedings of the fourth international conference on high levels of natural radiation: radiation doses and health effects, Beijing, China, pp 15–23
10. Paschoa A (2000) More than forty years of studies of natural radioactivity in Brazil. *Technology* 7(2–3):193–212
11. Kannan V (2002) Distribution of natural and anthropogenic radionuclides in soil and beach sand samples of Kalpakkam (India) using hyper pure germanium (HPGe) gamma ray spectrometry. *Appl Radiat Isot* 57(1):109–119. [https://doi.org/10.1016/S0969-8043\(01\)00262-7](https://doi.org/10.1016/S0969-8043(01)00262-7)
12. Ghiassi Nejad M (2002) Very high background radiation areas of Ramsar, Iran: preliminary biological studies. *Health Phys* 82(1):87–93
13. Wei L (2000) An introductory overview of the epidemiological study on the population at the high background radiation areas in Yangjiang, China. *J Radiat Res* 41(Suppl):S1–S7. <https://doi.org/10.1269/jrr.41.S1>
14. Sunta C (1993) A review of the studies of high background areas of the SW coast of India. In: Proceedings of the international conference on high levels of natural radiation, Ramsar, IAEA, pp 71–86
15. Radhakrishna A (1993) A new natural background radiation area on the southwest coast of India. *Health Phys* 65(4):390–395
16. Younis H (2022) Gamma radioactivity and environmental radiation risks of granitoids in central and western Gilgit Baltistan, Himalayas, North Pakistan. *Res Phys* 37:105509
17. Karam P (2001) The very high background radiation area in Ramsar, Iran: Public health risk or signal for a regulatory paradigm shift. pp 495–502

18. Kebwaro J (2011) Radiometric assessment of natural radioactivity levels around Mrima Hill, Kenya. 6(13): 3105–3110. <http://www.academicjournals.org/IJPS>
19. UNSCEAR (2000) United Nations scientific committee of the effect of atomic radiation (UNSCEAR). Sources, effects and risks of ionizing radiations. United Nations, New York
20. Bangotra P (2016) Study of natural radioactivity ( $^{226}\text{Ra}$ ,  $^{232}\text{Th}$  and  $^{40}\text{K}$ ) in soil samples for the assessment of average effective dose and radiation hazards. *Radiat Prot Dosimetry* 171(2):277–281. <https://doi.org/10.1093/rpd/ncw074>
21. Krewski D (2006) A combined analysis of North American case-control studies of residential radon and lung cancer. *J Toxicol Environ Health A* 69(7–8):533–597. <https://doi.org/10.1080/15287390500260945>
22. Darby S (2005) Radon in homes and risk of lung cancer: collaborative analysis of individual data from 13 European case control studies. *BMJ* 330(7485):223. <https://doi.org/10.1136/bmj.38308.477650.63>
23. Das B (2000) Cancer pattern in Haryana: twenty-one years experience. *Health Adm* 17(1):29
24. Chahal K (2022) Estimation of surface exhalation rate of thoron ( $^{220}\text{Rn}$ ) in soil samples of Aravalli Mountain range region of district Mahendergarh, Haryana, India using alpha detector Smart Rnduo. In: Proceedings of the DAE-BRNS symposium on Nuclear Physics V, pp 66
25. Nazaroff W (1992) Radon transport from soil to air. *Rev Geophys* 30(2):137–160. <https://doi.org/10.1029/92RG00055>
26. Sahu P (2013) Radon emanation from low-grade uranium ore. *J Environ Radioact* 126:104–114. <https://doi.org/10.1016/j.jenvrad.2013.07.014>
27. Kumar A (2014) Modeling of indoor radon concentration from radon exhalation rates of building materials and validation through measurements. *J Environ Radioact* 127:50–55. <https://doi.org/10.1016/j.jenvrad.2013.10.004>
28. Devi V (2019) A study on radionuclides content and radon exhalation from soil of Northern India. *Environ Earth Sci* 78:1–12. <https://doi.org/10.1007/s12665-019-8512-9>
29. Chauhan R (2016) Ventilation effect on indoor radon–thoron levels in dwellings and correlation with soil exhalation rates. *Indoor Built Environ* 25(1):203–212. <https://doi.org/10.1177/1420326X14542887>
30. Chauhan R (2011) Radon exhalation rates from stone and soil samples of Aravali hills in India. 9(1): 57–61
31. Mann N (2015) Radon-thoron measurements in air and soil from some districts of northern part of India. *Nucl Technol Radiat Protect* 30(4):294–300
32. Singh P (2016) Theoretical modeling of indoor radon concentration and its validation through measurements in South-East Haryana, India. *J Environ Manag* 171:35–41. <https://doi.org/10.1016/j.jenvman.2016.02.003>
33. Al-Shboul K (2023) Unraveling the complex interplay between soil characteristics and radon surface exhalation rates through machine learning models and multivariate analysis. *Environ Pollut*. <https://doi.org/10.1016/j.envpol.2023.122440>
34. Kanyan N (2020) Geochemistry and petrogenesis of Narnaul Pegmatites in Delhi Supergroup rocks, Narnaul area, southern Haryana, India. *J Nepal Geol Soc* 60:87–102. <https://doi.org/10.3126/jngs.v60i0.31268>
35. Ibrahiem N (1993) Measurement of radioactivity levels in soil in the Nile Delta and Middle Egypt. *Health Phys* 64(6):620–627
36. Saleh M (2014) Assessment of radiological health implicat from ambient environment in the Muar district, Johor, Malaysia. *Radiat Phys Chem* 103:243–252. <https://doi.org/10.1016/j.radphyschem.2014.05.054>
37. Melissinos A (2003) Experiments in modern physics. Gulf Professional Publishing
38. Durusoy A (2017) Determination of radioactivity concentrations in soil samples and dose assessment for Rize Province, Turkey. *J Radiat Res Appl Sci* 10(4):348–352. <https://doi.org/10.1016/j.jrras.2017.09.005>
39. Singh B (2021) Monitoring of natural radionuclides by alpha scintillometry and gamma spectrometry techniques in soil of district Palwal, Southern Haryana, India. *Int J Environ Anal Chem*. <https://doi.org/10.1080/03067319.2021.2016726>
40. Mann N (2018) Measurement of radium, thorium, potassium and associated hazard indices from the soil samples collected from Northern India. *Indoor Built Environ* 27(8):1149–1156. <https://doi.org/10.1177/1420326X17696136>
41. United Nations Scientific Committee on the Effects of Atomic Radiation (2000) Sources and Effects of Ionizing Radiation, United Nations Scientific Committee on the Effects of Atomic Radiation (UNSCEAR) 2000 Report, Volume I: Report to the General Assembly, with Scientific Annexes-Sources. United Nations
42. Beretka J (1985) Natural radioactivity of building materials, industrial wastes and byproducts. *Health Phys* 48:87–95
43. Guidebook A (1989) Measurement of radionuclides in food and the environment. International Atomic Energy Agency, Vienna
44. Joel E (2019) Investigation of natural environmental radioactivity concentration in soil of coastaline area of Ado Odo/Ota Nigeria and its radiological implications. *Sci Rep* 9(1):4219. <https://doi.org/10.1038/s41598-019-40884-0>
45. Saito K (1995) Gamma ray fields in the air due to sources in the ground. *Radiat Prot Dosimetry* 58(1):29–45. <https://doi.org/10.1093/oxfordjournals.rpd.a082594>
46. Gaware J (2011) Development of online radon and thoron monitoring systems for occupational and general environments. In the Forthcoming issue
47. Sahoo B (2007) Estimation of radon emanation factor in Indian building materials. *Radiat Meas* 42(8):1422–1425. <https://doi.org/10.1016/j.radmeas.2007.04.002>
48. Vaupotič J (1992) Alpha scintillation cell for direct measurement of indoor radon. *J Environ Sci Health Part A* 27(6):1535–1540
49. Porstendorfer J (1994) Properties and behaviour of radon and thoron and their decay products in the air. *J Aerosol Sci* 25(2):219–263. [https://doi.org/10.1016/0021-8502\(94\)90077-9](https://doi.org/10.1016/0021-8502(94)90077-9)
50. De Martino S (1998) Radon emanation and exhalation rates from soils measured with an electrostatic collector. *Appl Radiat Isot* 49(4):407–413. [https://doi.org/10.1016/S0969-8043\(96\)00300-4](https://doi.org/10.1016/S0969-8043(96)00300-4)
51. Kanse S (2013) Powder sandwich technique: a novel method for determining the thoron emanation potential of powders bearing high  $^{224}\text{Ra}$  content. *Radiat Meas* 48:82–87. <https://doi.org/10.1016/j.radmeas.2012.10.014>
52. Sahoo B (2014) Thoron interference in radon exhalation rate measured by solid state nuclear track detector based can technique. *J Radioanal Nucl Chem* 302:1417–1420. <https://doi.org/10.1007/s10967-014-3580-5>
53. Tuccimei P (2006) Simultaneous determination of  $^{222}\text{Rn}$  and  $^{220}\text{Rn}$  exhalation rates from building materials used in Central Italy with accumulation chambers and a continuous solid state alpha detector: influence of particle size, humidity and precursors concentration. *Appl Radiat Isot* 64(2):254–263. <https://doi.org/10.1016/j.apradiso.2005.07.016>
54. Poojitha C (2020) Assessment of radon and thoron exhalation from soils and dissolved radon in ground water in the vicinity of elevated granitic hill, Chikkaballapur district, Karnataka, India. *Radiat Prot Dosimetry* 190(2):185–192
55. Semwal P (2018) Measurement of  $^{222}\text{Rn}$  and  $^{220}\text{Rn}$  exhalation rate from soil samples of Kumaun Hills, India. *Acta Geophys* 66(5):1203–1211

56. Kaur M (2021) Measurement of radionuclide contents and  $^{222}\text{Rn}/^{220}\text{Rn}$  exhalation rate in soil samples from the sub-mountainous region of India. *Arab J Geosci* 14(9):1–16
57. Kaur M (2018) Study of radon/thoron exhalation rate, soil-gas radon concentration, and assessment of indoor radon/thoron concentration in Siwalik Himalayas of Jammu & Kashmir. *Hum Ecol Risk Assess Int J* 24(8):2275–2287
58. Chauhan R (2014) Estimation of dose contribution from  $^{226}\text{Ra}$ ,  $^{232}\text{Th}$  and  $^{40}\text{K}$  radon exhalation rates in soil samples from Shivalik foot hills in India. *Radiat Prot Dosimetry* 158(1):79–86
59. Babu P (1993) Tin and Rare Metal Pegmatites of the Bastar-Koraput Pegmatite Belt, Madhya Pradesh and Orissa, India. Characterisation and Classification. *Geol Soc India* 42(2):180–190
60. Kumar P (2019) Itacolumite (Flexible sandstone) from Kaliana, Charkhi Dadri District, Haryana, India. *J Geol Soc India* 93:278–284
61. Dina NT (2022) Natural radioactivity and its radiological implications from soils and rocks in Jaintiapur area, North-east Bangladesh. *J Radioanal Nucl Chem* 331(11):4457–4468
62. Akhtaruzzaman M (2014) Morphological, physical and chemical characteristics of hill forest soils at Chittagong University, Bangladesh. *Open J Soil Sci* 4:26–35. <https://doi.org/10.4236/ojss.2014.41004>
63. Chowdhury CR (2020) Radionuclide activity concentration in soil, granites and water in a fluorosis endemic area of India: an oral health perspective. *J Oral Biol Craniofacial Res* 10(3):259–262
64. Yadav S (2019) Fluoride distribution in underground water of district Mahendergarh, Haryana, India. *Appl Water Sci* 9:1–11

**Publisher's Note** Springer Nature remains neutral with regard to jurisdictional claims in published maps and institutional affiliations.

Springer Nature or its licensor (e.g. a society or other partner) holds exclusive rights to this article under a publishing agreement with the author(s) or other rightsholder(s); author self-archiving of the accepted manuscript version of this article is solely governed by the terms of such publishing agreement and applicable law.